Study of systematics related to readout electronics in liquid argon TPC detectors for the SBN Program

ANDREA SERAFINI

27 Sept. 2017

CONTENTS

ABSTRACT

The Short-Baseline Neutrino (SBN) Program is a short-baseline neutrino oscillation experiment in the Booster Neutrino Beam-line (BNB) at Fermilab. It consists of three Liquid Argon Time Projection Chambers (LArTPCs): the Short-Baseline Near Detector (SBND), Micro Booster Neutrino Experiment (MicroBooNE), and Imaging Cosmic And Rare Underground Signals (ICARUS) detectors. The SBN Program will search for short-baseline neutrino oscillations for investigating the possible existence of new sterile neutrino states, make precision neutrino-argon interaction measurements, and further develop the LArTPC technology[1].

In order to maximize the overall sensitivity of the SBN Program to neutrino oscillation studies, a careful investigation of possible systematics contributions due to differences in between the detectors needs to be carried out.

In this article results of the study of different configurations of the readout electronics are reported.

* *Department of Physics, University of Ferrara, Italy*

1 NEUTRINO PHYSICS

Neutrinos were introduced in the Standard Model as electrically neutral, massless and weakly interacting leptons, one for each family (ν_e, ν_μ and ν_τ). However, experiments in the last decades showed in a incontrovertible way that neutrinos can oscillate between flavor states and therefore have a mass. This happens because of the non correspondence between mass and flavor eigenstates. Each flavor state is a superposition of different mass states, its evolution in time depends on the distance at witch the neutrino is observed, its energy and its mass. The probability of oscillation is $P \propto \sin^2(\frac{\Delta m^2 L}{E})$, where $\Delta m^2 = m_b^2 - m_a^2$ is the difference between the squared masses of two states. By varying the distance from the source (baseline) and the beam energy, it is possible to explore a broad parameter space for Δm^2. Two clearly separated oscillation regimes have been experimentally observed in the last decades, corresponding to $\Delta m^2_{atm} \sim 2 \times 10^{-3}$ eV^2 and $\Delta m^2_{sol} \sim 7 \times 10^{-5}$ eV^2[2].

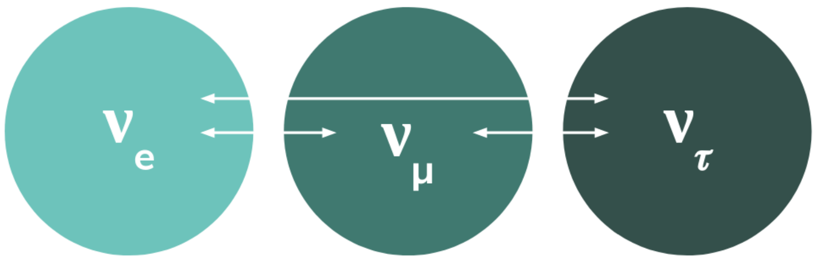

2 THE EXPERIMENT

A series of experimental anomalies, uncorrelated with each other but all hinting at oscillation phenomena driven by values of the Δm^2 parameter not compatible with the values reported in the previous paragraph, has started casting shadows over the picture of 3 generations of neutrinos since the late 90's. In particular observation of ν_e interactions in ν_μ beams produced at accelerators and propagated over short baselines, well beyond the intrinsic beam contamination, have been reported by LSND[3] and MiniBooNE[4] experiments, indicating $\Delta m^2 \sim 1$ eV^2. One plausible explanation, still without entering in conflict with the precision measurements of the decay width of Z^0 boson that limit the number of active light neutrinos to 3[5], is the existence of one or more additional sterile (i.e. not weakly interacting) neutrino states.

The Short Baseline Neutrino (SBN) Program has been approved in 2015 with the intent of confirming or ruling out this hypothesis. The experiment will also contribute to the development of LArTPC technology for the long-baseline DUNE[6] experiment planned to be operational in 2027.

The Program consists of three different LArTPC detectors along the ν_μ Booster Neutrino Beam-line (BNB) at Fermilab.

The strong point is the possibility to track the oscillation measuring the disappearance of ν_μ in the neutrino flux, and at the same time the ν_e appearance.

ICARUS is the farthest detector of the program. It is composed of two semi-independent cryostats, holding 2 liquid argon time projection chambers each. It is located at a distance of 600 m from the neutrino source, where the sterile neutrino oscillation should be maximum. It is the largest of the three detectors, with 500 tons of liquid argon in the active volumes. ICARUS arrived from CERN on July 26 and is now under installation.

MICROBOONE is the central detector of the three. Placed at a distance of 470 m from the source it consists of a liquid argon time projection chamber, with 80 tons of liquid argon in the active volume. It is located in the exact same place where MiniBooNE took place, in order to try to explain its anomalies. The cryostat was filled in 2015 and the detector is currently operating. This data will produce neutrino cross section measurements, useful for future experiments, such as DUNE and the SBN program.

SBND is the nearest detector. It will be a 112 tons active volume liquid argon time projection chamber to be located only 110 m from the neutrino source. The detector is currently in the design phase. SBND will record over a million neutrino interactions per year. By providing such a high statistics measurement of the un-oscillated content of the booster neutrino beam, SBND is a critical element in performing searches for neutrino oscillations.

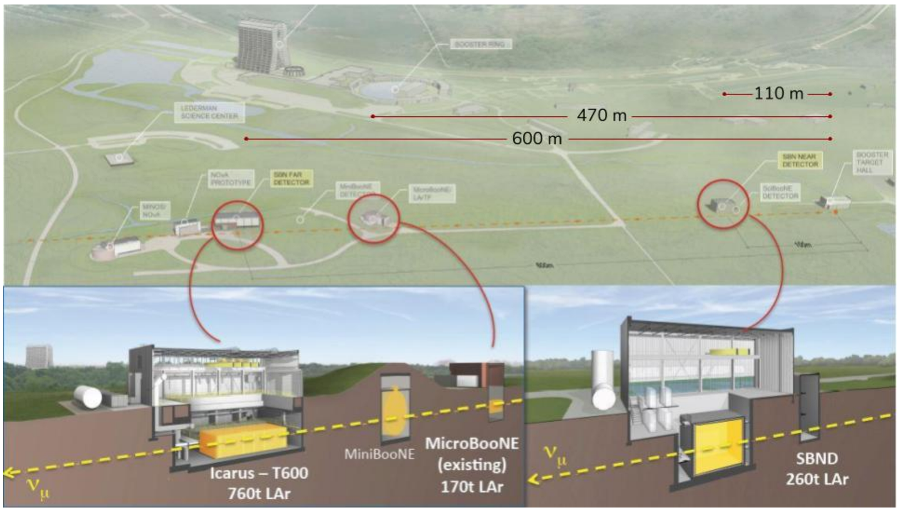

Figure 1: Map of the detectors in SBN

3 LARTPC TECHNOLOGY

All detectors in the SBN program are going to use the same technology, that is the Liquid Argon Time Projection Chamber.
LArTPC detectors represent a modern take on the successful Bubble Chamber technology: they preserve a high resolution imaging with the additional features of scalability up to large masses and electronic processing of the data. This makes them one of the best detectors for neutrino physics.

Incoming charged particles, if energetic enough, can ionize Argon atoms (ionization energy ~ 16 eV [7]). A drift field drives the electrons through one or more *induction planes* towards a *collection plane* made of wires.
Since the electron velocity is constant, combining the information on the wire number and electrons' time of arrival a 2D trajectory can be reconstructed. A full 3D image can be obtained by matching the multiple projections for each plane using the common drift coordinate.

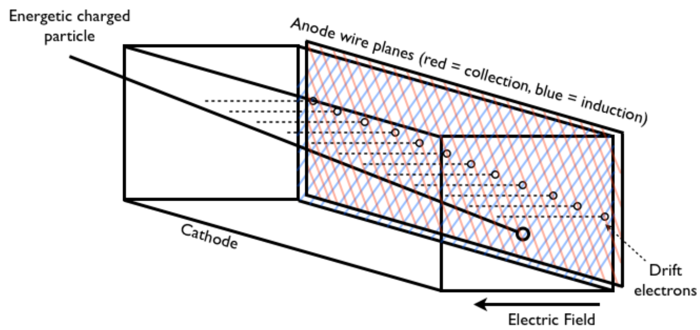

Figure 2: Simple scheme of a typical LArTPC

4 DIFFERENCES BETWEEN DETECTORS

An effective neutrino oscillation search in the framework of the SBN Program requires a combined analysis of data collected with the three detectors. Therefore any possible difference among the detectors need to be carefully examined, because it could affect the final sensitivity of the Program.

WIRES ORIENTATION is different for the detectors. ICARUS is using two induction planes at $\pm\ 60°$ and a collection plane with $0°$ wires.
MicroBooNE has two induction planes at $\pm\ 60°$, but the collection plane is vertical at $90°$. SBND is going to use the same configuration.

ELECTRIC FIELD All three detectors are going to use different values for the drift field (between 0.1 kV/cm and 0.5 kV/cm) and this will change the drift velocity for electrons. The time and space resolutions are going to be affected by this. Also, despite the fields should be homogeneous for all detectors, small inhomogeneities are unavoidable, and these will differ detector by detector. One of possible sources of uniformities is the spatial charge caused by heavy positive ions, that because of their higher mass (with respect to electrons) move slowly towards the anode, altering the electric field.

ARGON PURITY Detectors in the SBN collaboration may have different levels of purity for liquid Argon. This can affect the fraction of electron absorbed during the drift, putting a systematic on the energy reconstruction.

ACTIVE VOLUME Detectors will have different volumes. This is going to affect the number of measured neutrino interactions for each LArTPC.

TPC READOUT ELECTRONICS All detectors will differ in the readout electronics, both the placement and the functioning parameters:

1. the **preamplifier** is placed outside the detector for ICARUS,while it is inside for MicroBooNE/SBND. This is going to affect the electronic noise on the signal.
2. detectors have different **shapers** (see par.6). This could in principle affect the topology and the calorimetry.
3. the **sampling** frequency (see par.7) of the digitizer is going to be slightly different for the detectors. This may affect the time resolution in the signal and the calorimetry as well.

My internship activity was mainly focused on investigating the impact of shaping and sampling parameters on data analysis.

5 LARIAT DATA

In order to better focus on effects of the electronic processing of TPC signals, disentangling them from other detector-related effects, still taking into account the possible impact of realistic electronic noise conditions, the analysis has been carried out on a sample of data collected with the LArIAT[8] detector. LArIAT is a small LArTPC dedicated to a full physics program on hadron-argon interaction measurements which are of high importance to understand both secondary interactions and final state processes in neutrino-argon experiments and to the calibration and the characterization of output responses for SBN detectors. It shares all the readout electronics with MicroBooNE and it is easier to study because of its small volume. Electronic noise is negligible for LArIAT data, allowing to focus exclusively on electronics. Data acquisitions with different configuration of the parameters of readout electronics have been performed and are now under study.
In order to study these datasets, events have been selected according to 4 possible different topologies:

- Single tracks (284 events);
- Multiple tracks (121 events);
- Delta rays (208 events);
- Showers (123 events);

A graphic example for each category can be observed in Fig.3.

6 SHAPING

A relevant component of the analogue processing of the signals coming from TPC wires is the shaper, which, using a series of differentiating and integrating circuits amplifies the signal and gives it a different shape.
By integrating over a commensurate period of time, the shaper is able to strongly reduce the noise on the signal: in fact white noise is random in time and, over a period, contributions cancel out.
The flip side of the coin is that extending the integration window causes a worsening of the time resolution of the output signal, and therefore a degradation of the topological reconstruction of particle tracks.
The careful tuning of the balancing between these two effects is detector

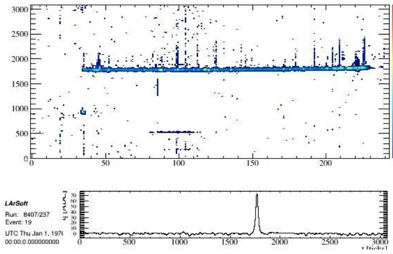

(a) Single track

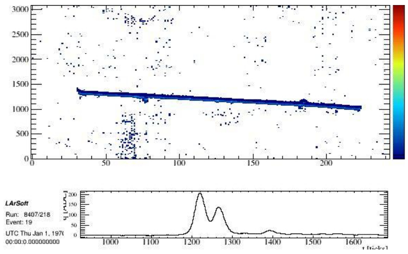

(b) Delta ray

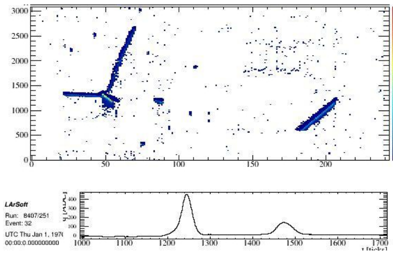

(c) Multiple track

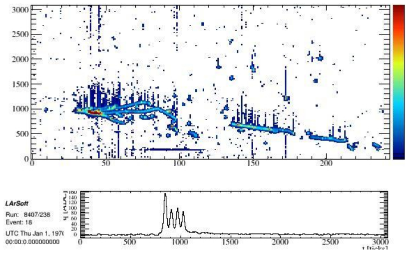

(d) Shower

Figure 3: Different categories of analyzed events

specific, and heavily depends on the experimental conditions, particularly the level of noise. Detectors in the SBN program are using gaussian shapers

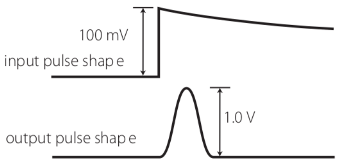

(a) Shaped analog signal.

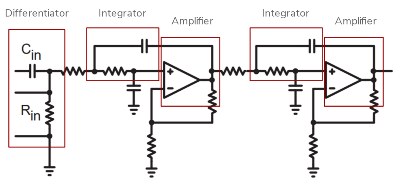

(b) Simple scheme of a shaper.

(Fig.4a): the shaping time is the time constant of the circuit, and it is proportional to the width of the generated signal.

Simulation

In order to better understand the behavior of the shaper on the signal and the impact it could have on data, a simulation has been developed.
A random amount of charge is generated in a point in time and then transformed into a gaussian-like signal. This process is performed using different shaping times parameters, that have been chosen to be 1.0 µs and 2.0 µs to match the ones for available data (see Fig.4).

Data analysis

For the study on shaping time, two sets of data at 1.0 µs and 2.0 µs have been analyzed. Both the two sets were sampled at 256ns.
The data analysis is focused on two studies:

- Time resolution;
- Calorimetry;

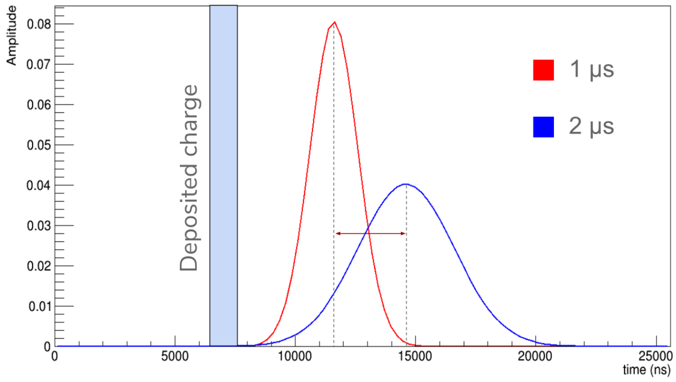

Figure 4: Example of simulated signals whit different shaping parameters.

Since studying exactly the same events with different shaping parameters was not possible, a statistical study had to be performed.

6.0.1 *Time resolution*

For studying the impact on time resolution, all categories of events (see Fig.3) were taken into account. The distance between two consecutive hits in the same wire was plotted in an histogram to understand how the minimum discernible distance between hits was affected by the shaping parameter. From Fig.5b it can be observed that the distributions are different for the two data sets*, but the starting points of the curves are similar, meaning that the minimum distance between peaks is the same for the two shaping times. This means that the shaping time is not affecting time resolution within our hit reconstruction sensitivity.

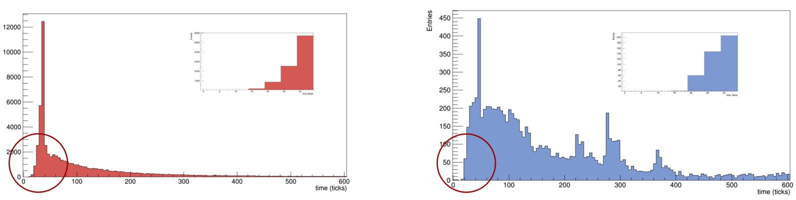

(a) Distance between peaks at 1.0 µs **(b)** Distance between peaks at 2.0 µs

**possible explanations for this are:*

- *having different shaping times means having different levels of noise. For* 1.0 µs *the noise level is higher, and more random peaks could be recognized as hits, reducing the distance between peaks on average;*
- *different parameters in the beam (energy, intensity etc.) may affect the probability of having certain types of event with respect to others;*

6.0.2 *Calorimetry*

For the calorimetry study, single muon tracks (see Fig.3a) have been analyzed. Two histograms have been filled with the area for each hit for the two different data sets, which is proportional to the deposited energy of the incoming particle (after a calibration). Fig.5a shows that the behavior is the same for both the shaping times. The MPV is (539 ± 6) ADCcounts for the first histogram and (546 ± 8) ADCcounts for the second one, confirming that the distributions are comparable. In Fig.5c from the superimposition of the 2 functions it can be observed that also calorimetry seems not to be affected by shaping time.

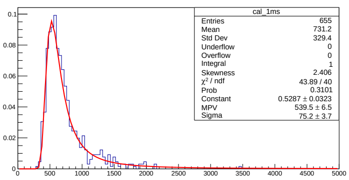

(a) Hits integral distribution at 1.0 μs

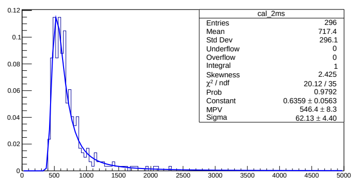

(b) Hits integral distribution at 2.0 μs

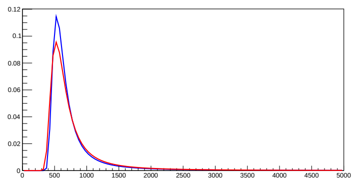

(c) Landau fits

7 SAMPLING

The analogue signal processing is followed by the digitalisation by means of Analogue-to-digital converters (ADC), whose functioning rate determines the sampling time, i.e. the time difference between two consecutive samples.
Once an analog signal enters a sampler, a set of values at different points in time is taken. The signal is assumed constant for the entire period between two consecutive samples.

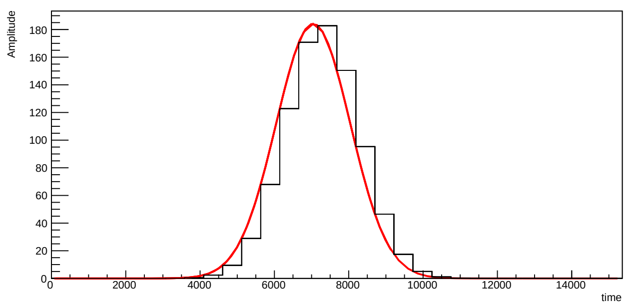

Figure 5: Sampling of an analog gaussian signal (red).

The sampling time parameter can heavily affect the shape of the signal. A good choice of the sampling time is essential to preserve the original signal shape, without loosing to much information.
As can be observed in Fig.5, sampling a signal can affect its characteristic, such as the peak time or the underlying area. Also the choice of the sampling time has to take into account the width: using a large sampling time would mean have a bad replication of the signal, using a small one would mean dealing with big amounts of data.

Simulation

To better understand the behavior of the sampling process, and to be able to interpret the results from data analysis, a simulation over the sampling of gaussian analog signals was coded and run. A random analog gaussian-like signal (previously shaped) is sampled using two different sampling times. In order to match the available data from LArIAT these parameters were chosen to be 256 ns and 512 ns. The sampled signal is then refitted with a gaus function to replicate the hit reconstruction used in LArIAT experiment. As you can see in Fig.6 the peak time and the hit underlying area can be affected by the sampling. These quantities have then been compared to the ones extracted from data.

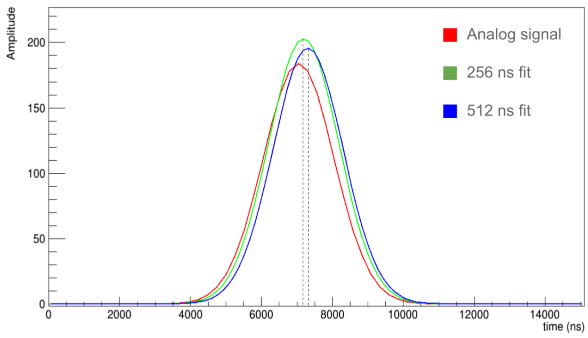

Figure 6: Example of analog signals sampled and refitted with different sampling times.

Data analysis

For the study on sampling time, a set of data sampled at 256 ns has been chosen. A second set of data at 512 ns has been obtained by software by skipping half of the samples.
The data analysis is focused on two studies:

- Time resolution;
- Calorimetry;

Since the second set of data at 512 ns has been obtained by software, the two datasets contain exactly the same data, but with different sampling times. A comparison event-by-event was possible.

7.0.3 *Time resolution*

For the time resolution study more than 210 delta rays have been chosen by looking by eye at the events. The distance between the electron delta ray track and the main muon track has been plotted in an histogram for each wire. To do this, an algorithm had to be developed in order to match the same hits in the two different datasets. As can be seen in Fig.7b the distribution is the same for both the sampling times. Also the minimum discernible distance, that can be obtained by the starting point of the distribution is exactly the same, independently by the the sampling time.
Therefore different parameters for the sampling time seem non to affect the time resolution we have on distinguish peaks.

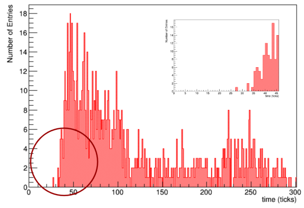

(a) Distance between peaks at 256 ns

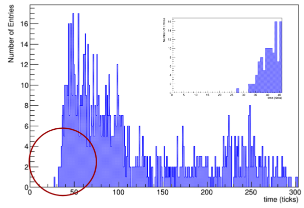

(b) Distance between peaks at 512 ns

7.0.4 *Calorimetry*

For a calorimetry study all categories of events have been analyzed. More than 750 events have been chosen and divided in categories by eye. Histograms have been filled with the area for each hit for the two different data sets, which is proportional to the deposited energy of the incoming particle. Each category of events has been studied separately. As you can see from

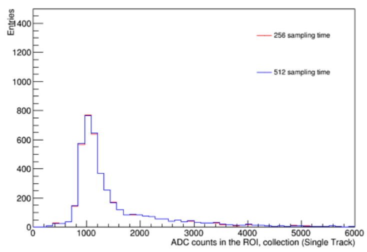

(a) Single track

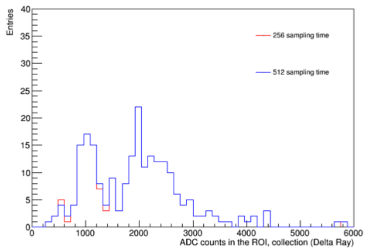

(b) Delta ray

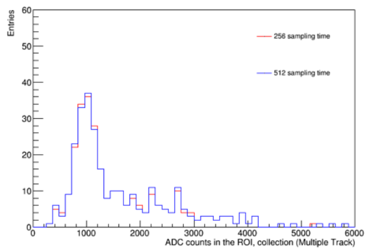

(c) Multiple track

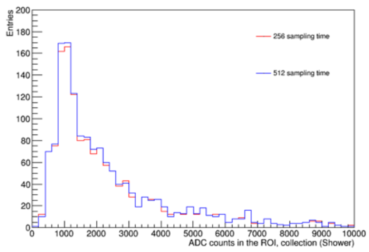

(d) Shower

Figure 7: Sampling effect on calorimetry.

Fig.7 the superimposed distributions for two different sampling times are consistent for all the categories. The calorimetry seems not to be affected by the different sampling parameters.

8 RESULTS AND DISCUSSION

The analysis of possible impacts of different configurations of the readout electronics, hereby reported, showed no effect neither of the shaping nor of the sampling time on calorimetric and tracking performance of LArTPC detectors.
Despite similarity in the general behavior, some differences arose when comparing data event-by-event. A careful study focused on these differences showed some issues with LArSoft, a software used for analysis in LArTPC experiments, that helps to perform better developments on how to make such software framework more modular and effective for the different LArTPC experiments. It was discovered that most of the differences are not due to a different physical behavior, but to intrinsic behavior of the deconvolution of the signal and the hit finder algorithm. Those results are relevant to the SBN Program and can certainly contribute to a better understanding of detector relate systematics. Particular thanks to LArIAT collaboration for their support during these studies and the data provided, that have been used for this analysis.

REFERENCES

[1] M. Bass. The Short Baseline Neutrino Oscillation Program at Fermilab. *ArXiv e-prints*, February 2017.

[2] Neutrino mass, mixing and oscillation. *http://pdg.lbl.gov/2017/reviews/rpp2016-rev-neutrino-mixing.pdf*.

[3] A. Aguilar, L. B. Auerbach, R. L. Burman, D. O. Caldwell, E. D. Church, A. K. Cochran, J. B. Donahue, A. Fazely, G. T. Garvey, R. M. Gunasingha, R. Imlay, W. C. Louis, R. Majkic, A. Malik, W. Metcalf, G. B. Mills, V. Sandberg, D. Smith, I. Stancu, M. Sung, R. Tayloe, G. J. Vandalen, W. Vernon, N. Wadia, D. H. White, and S. Yellin. Evidence for neutrino oscillations from the observation of ν_e appearance in a ν_μ beam. , 64(11):112007, December 2001.

[4] A. A. Aguilar-Arevalo et al. (MiniBooNE Collaboration). Improved Search for ν_e to ν_μ beam oscillations in the MiniBooNE Experiment. April 2013.

[5] The ALEPH Collaboration, the DELPHI Collaboration, the L3 Collaboration, the OPAL Collaboration, the SLD Collaboration, the LEP Electroweak Working Group, t. SLD electroweak, and heavy flavour groups. Precision Electroweak Measurements on the Z Resonance. *ArXiv High Energy Physics - Experiment e-prints*, September 2005.

[6] J. Strait, E. McCluskey, T. Lundin, J. Willhite, T. Hamernik, V. Papadimitriou, A. Marchionni, M. J. Kim, M. Nessi, D. Montanari, and A. Heavey. Long-Baseline Neutrino Facility (LBNF) and Deep Underground Neutrino Experiment (DUNE) Conceptual Design Report Volume 3: Long-Baseline Neutrino Facility for DUNE June 24, 2015. *ArXiv e-prints*, January 2016.

[7] Argon ionization energy. *https://www.nist.gov/pml*.

[8] J. Paley, D. Gastler, E. Kearns, R. Linehan, R. Patterson, W. Foremen, J. Ho, D. Schmitz, R. Johnson, J. St. John, R. Acciarri, P. Adamson, M. Backfish, W. Badgett, B. Baller, A. Hahn, D. Jensen, T. Junk, M. Kirby, T. Kobilarcik, P. Kryczynski, H. Lippincott, A. Marchionni, K. Nishikawa, J. Raaf, E. Ramberg, B. Rebel, M. Stancari, G. Zeller, M. Wascko, T. Maruyama, E. Iwai, S. Kunori, C. Mauger, F. Blaszczyk, W. Metcalf, A. Olivier, M. Tzanov, J. Evans, P. Guzowski, C. Bromberg, D. Edmunds, D. Shooltz, R. Gran, A. Habig, K. Kaess, S. Dytman, J. Asaadi, M. Soderberg, J. Esquivel, A. Farbin, S. Park, J. Yu, J. Huang, K. Lang, R. Nichol, A. Holin, J. Thomas, M. Kordosky, M. Stephens, P. Vahle, B. T. Fleming, F. Cavanna, E. Church, E. Gramellini, O. Palamara, and A. Szelc. LArIAT: Liquid Argon In A Testbeam. *ArXiv e-prints*, June 2014.